J Nonlinear Sci (2012) 22:499–515
DOI 10.1007/s00332-012-9142-5

Journal of
Nonlinear
Science

Energy-Momentum Stability of Icosahedral Configurations of Point Vortices on a Sphere

Paul K. Newton · Vitalii Ostrovskyi

Received: 7 November 2011 / Accepted: 28 June 2012 / Published online: 19 July 2012

Abstract We investigate the nonlinear stability of the icosahedral relative equilibrium configuration of point vortices on a sphere. The relative equilibrium problem is formulated as a problem of finding the nullspace of the configuration matrix that encodes the geometry of the icosahedron, as in Jamaloodeen and Newton (Proc. Royal Soc. A, Math. Phys. Eng. Sci. 462(2075):3277, 2006). The seven-dimensional nullspace of the configuration matrix, **A**, associated with the icosahedral geometry gives rise to a basis set of vortex strengths for which the icosahedron stays in relative formation, and we use these values to form the augmented Hamiltonian governing the stability. We choose the basis set made up of (i) one element with equal strength vortices on every vertex of the icosahedron (the uniform icosahedron); (ii) six elements made up of equal and opposite antipodal pairs. We start by proving nonlinear stability of the antipodal vortex pair (by direct methods). Following the methods laid out in Simo et al. (Arch. Ration. Mech. Anal. 115(1):15–59, 1991) and Pekarsky and Marsden (J. Math. Phys. 39(11):5894–5907, 1998) and more generally in Marsden and Ratiu (Introduction to Mechanics and Symmetry, 1999), we then combine our knowledge of the nullspace structure of **A** with the structure of the underlying Hamiltonian, and analyze the stability of the icosahedron using the energy-momentum method. Because the parameter space is large, we focus on the physically motivated and important case obtained by combining the basis elements into (i) the uniform icosahedron; (ii) a von Kármán vortex street configuration of equal and opposite staggered, evenly

Communicated by Anthony Bloch.

P.K. Newton (✉) · V. Ostrovskyi
Department of Aerospace & Mechanical Engineering and Department of Mathematics, University of Southern California, Los Angeles, CA 90089-1191, USA
e-mail: newton@usc.edu

spaced latitudinal rows equidistant from the equator (Chamoun et al. in Phys. Fluids 21:116603, 2009), and (iii) the North Pole–South Pole equal and opposite vortex pair. Stability boundaries in a three-parameter space are calculated for linear combinations of these grouped basis configurations.

Keywords Stability of point vortices · Relative equilibria · Point vortex equilibria · Energy-momentum method

Mathematics Subject Classification 76B47 · 70H14 · 70E50 · 37N10 · 37J25

1 Introduction to the Equations of Motion

Consider the system of N point vortices on a spherical shell of ideal incompressible fluid. Each point vortex can occupy any position on the sphere except positions of the other point vortices. Thus, the phase space of the system can be described as N copies of 2-spheres without points $x_i = x_j$, $1 \le i < j \le N$:

$$P = \{(x_1, x_2, \dots, x_N) \in S^2 \times S^2 \times \cdots \times S^2 \,|\, x_i \neq x_j, i \neq j\}.$$

The equations of motion of N point vortices take the following form (see Bogomolov 1977; Kimura and Okamoto 1987; Newton 2001):

$$\begin{aligned} \sin\theta_i \dot{\phi}_i &= -\frac{1}{4\pi r^2} \sum_{j=1, i\neq j}^{N} \Gamma_j \frac{\kappa_{ij}}{1-\cos\gamma_{ij}}, \\ \dot{\theta}_i &= -\frac{1}{4\pi r^2} \sum_{j=1, i\neq j}^{N} \Gamma_j \frac{\sin\theta_j \sin(\phi_i - \phi_j)}{1-\cos\gamma_{ij}}, \end{aligned} \tag{1.1}$$

where (ϕ_i, θ_i) are the spherical coordinates of the ith point vortex, r is the radius of a sphere, γ_{ij} is the central angle between point vortices ($\cos\gamma_{ij} = \cos\theta_i \cos\theta_j' + \sin\theta_i \sin\theta_j \cos(\phi_i - \phi_j)$), and $\kappa_{ij} = \cos\theta_i \sin\theta_j \cos(\phi_i - \phi_j) - \sin\theta_i \cos\theta_j$.

The Hamiltonian structure behind (1.1) is given by

$$\begin{aligned} \mathcal{H}_s &= -\frac{1}{4\pi r^2} \sum_{i<j} \Gamma_i \Gamma_j \ln l_{ij}, \\ p_i &= \sqrt{|\Gamma_i|}\cos\theta_i, \qquad q_i = \operatorname{sign}(\Gamma_i)\sqrt{|\Gamma_i|}\phi_i, \\ \dot{p}_i &= -\frac{\partial \mathcal{H}_s}{\partial q_i}, \qquad \dot{q}_i = \frac{\partial \mathcal{H}_s}{\partial p_i}, \end{aligned} \tag{1.2}$$

where $l_{ij}^2 = (\mathbf{x}_i - \mathbf{x}_j)^2 = 2r^2(1 - \cos\gamma_{ij})$.

As we can see from the form of canonical variables, it is useful to rewrite the Hamiltonian in cylindrical coordinates $z = r\cos\theta$, $\phi = \phi$:

$$\mathcal{H}_s = -\frac{1}{4\pi r^2} \sum_{i<j} \Gamma_i \Gamma_j \ln\Big[2\Big(1 - z_i z_j - \sqrt{r^2 - z_i^2}\sqrt{r^2 - z_j^2}\cos(\phi_i - \phi_j)\Big)\Big]. \tag{1.3}$$

Since both spherical and cylindrical coordinates are singular at the poles, the motion in their vicinity is best described using cartesian coordinates. The Hamiltonian in this mixed chart can be represented as

$$\begin{aligned}\mathcal{H}_m = -\frac{1}{4\pi r^2}\Bigg(&\sum_{1\le i<j\le N} \Gamma_i\Gamma_j \ln\Big[2\Big(1 - z_i z_j - \sqrt{r^2-z_i^2}\sqrt{r^2-z_j^2}\cos(\phi_i-\phi_j)\Big)\Big]\\ &+\sum_{i=1}^{i=N}\Gamma_i\Gamma_s \ln\Big[2\Big(1-\sqrt{r^2-z_i^2}(x_s\cos\phi_i + y_s\sin\phi_i) - z_s z_i\Big)\Big]\\ &+\sum_{i=1}^{i=N}\Gamma_i\Gamma_n \ln\Big[2\Big(1-\sqrt{r^2-z_i^2}(x_n\cos\phi_i + y_n\sin\phi_i) - z_n z_i\Big)\Big]\\ &+\Gamma_s\Gamma_n \ln\big[2(1-x_s x_n - y_s y_n - z_s z_n)\big]\Bigg),\end{aligned} \tag{1.4}$$

where (x_s, y_s, z_s), (x_n, y_n, z_n) are coordinates of point vortices in the vicinity of the South and North poles, respectively, and Γ_s, Γ_n their intensities. Then, the equations of motion of the point vortices near the poles can be written as

$$\dot{x}_s = -\frac{z_s}{\Gamma_s}\frac{\partial\mathcal{H}_m}{\partial y_s}, \qquad \dot{y}_s = \frac{z_s}{\Gamma_s}\frac{\partial\mathcal{H}_m}{\partial x_s},$$
$$\dot{x}_n = -\frac{z_n}{\Gamma_n}\frac{\partial\mathcal{H}_m}{\partial y_n}, \qquad \dot{y}_n = \frac{z_n}{\Gamma_n}\frac{\partial\mathcal{H}_m}{\partial x_n}.$$

Notice that z_n and z_s are not independent variables; they are functions of x_s, y_s, x_n, y_n:

$$z_s = -\sqrt{r^2 - x_s^2 - y_s^2},$$
$$z_n = \sqrt{r^2 - x_n^2 - y_n^2}.$$

If we embed the sphere into $\mathbb{R}^3$ and use vectors $\mathbf{x}_i$, $1 \le i \le N$ to represent the positions of the point vortices, the equations of motion become (see Newton 2001):

$$\begin{aligned}\dot{\mathbf{x}}_i &= \sum_{j=1, j\ne i}^{N} \frac{\Gamma_j}{2\pi r}\frac{\mathbf{x}_j\times\mathbf{x}_i}{(\mathbf{x}_i-\mathbf{x}_j)^2},\\ \|x_i\|^2 &= r^2, \quad \forall 0\le i\le N.\end{aligned} \tag{1.5}$$

It is shown in Jamaloodeen and Newton (2006) that the equations of motion can be reduced to equations for the inter-vortical distances $l_{ij} = |\mathbf{x}_i - \mathbf{x}_j|^2$, $1 \le i < j \le N$. To obtain this form of the equations, subtract the equation of motion of the ith from the jth vortex, and dot multiply the difference by $(\mathbf{x}_i - \mathbf{x}_j)$. This gives

$$
\begin{aligned}
&(\dot{\mathbf{x}}_i - \dot{\mathbf{x}}_j) \cdot (\mathbf{x}_i - \mathbf{x}_j) \\
&\quad = \sum_{k=1, k\neq i, k\neq j}^{N} \frac{\Gamma_k}{2\pi r} \left[\frac{(\mathbf{x}_k \times \mathbf{x}_i) \cdot (\mathbf{x}_i - \mathbf{x}_j)}{(\mathbf{x}_i - \mathbf{x}_k)^2} - \frac{(\mathbf{x}_k \times \mathbf{x}_j) \cdot (\mathbf{x}_i - \mathbf{x}_j)}{(\mathbf{x}_j - \mathbf{x}_k)^2} \right] \\
&\qquad + \frac{\Gamma_j}{2\pi r} \frac{(\mathbf{x}_j \times \mathbf{x}_i) \cdot (\mathbf{x}_i - \mathbf{x}_j)}{(\mathbf{x}_i - \mathbf{x}_j)^2} - \frac{\Gamma_i}{2\pi r} \frac{(\mathbf{x}_i \times \mathbf{x}_j) \cdot (\mathbf{x}_i - \mathbf{x}_j)}{(\mathbf{x}_j - \mathbf{x}_i)^2} \\
&\quad = \sum_{k=1, k\neq i, k\neq j}^{N} \frac{\Gamma_k}{2\pi r} \left[\frac{\mathbf{x}_i \cdot \mathbf{x}_j \times \mathbf{x}_k}{(\mathbf{x}_j - \mathbf{x}_k)^2} - \frac{\mathbf{x}_i \cdot \mathbf{x}_j \times \mathbf{x}_k}{(\mathbf{x}_i - \mathbf{x}_k)^2} \right] \\
&\quad = \sum_{k=1, k\neq i, k\neq j}^{N} \frac{\Gamma_k}{2\pi r} \left[\frac{\mathbf{x}_i \cdot \mathbf{x}_j \times \mathbf{x}_k}{(\mathbf{x}_j - \mathbf{x}_k)^2} - \frac{\mathbf{x}_i \cdot \mathbf{x}_j \times \mathbf{x}_k}{(\mathbf{x}_i - \mathbf{x}_k)^2} \right].
\end{aligned}
$$

Since $\frac{\mathrm{d}l_{ij}^2}{\mathrm{d}t} = 2(\dot{\mathbf{x}}_i - \dot{\mathbf{x}}_j) \cdot (\mathbf{x}_i - \mathbf{x}_j)$, then

$$
\frac{\mathrm{d}l_{ij}^2}{\mathrm{d}t} = \sum_{k=1, k\neq i, k\neq j}^{N} \frac{\Gamma_k V_{ijk}}{\pi r} \left(\frac{1}{l_{jk}^2} - \frac{1}{l_{ik}^2} \right), \tag{1.6}
$$

where $V_{ijk} = \mathbf{x}_i \cdot \mathbf{x}_j \times \mathbf{x}_k$. These equations depend only on l_{ij}^2 and describe the relative motion of point vortices on a sphere.

Since the Hamiltonian depends only on quantities invariant under spherical rotations (l_{ij}^2), it is invariant under action of the group SO(3). According to Noether's theorem (Marsden and Ratiu 1999), because of this symmetry, the system has $\dim(\mathrm{SO}(3)) = 3$ conserved scalar quantities. Following Marsden and Ratiu (1999) and Pekarsky and Marsden (1998), we can find these quantities as components of the *momentum map* $\mathbf{J}$:

$$
\begin{aligned}
J_1 &= \frac{1}{r} \sum_{i=1}^{N} \Gamma_i x_i = \sum_{i=1}^{N} \Gamma_i \sin\theta_i \cos\phi_i = \text{const.}, \\
J_2 &= \frac{1}{r} \sum_{i=1}^{N} \Gamma_i y_i = \sum_{i=1}^{N} \Gamma_i \sin\theta_i \sin\phi_i = \text{const.}, \\
J_3 &= \frac{1}{r} \sum_{i=1}^{N} \Gamma_i z_i = \sum_{i=1}^{N} \Gamma_i \cos\theta_i = \text{const.}
\end{aligned} \tag{1.7}
$$

The vector $\mathbf{J} = (J_1, J_2, J_3)$ is sometimes called the *center of vorticity*, and it is shown in Newton (2001) to be a conserved quantity. It is a key quantity used in the analysis of Kidambi and Newton (1998) in their solution of the three-vortex problem on the sphere.

The general literature on point vortex dynamics is large (see Newton 2001, for an entry), but the more targeted work focusing on the sphere is much smaller (although growing) and more recent, motivated mostly by atmospheric and geophysical applications where the spherical geometry plays a central role (see, for example, Polvani and Dritschel 1993; Humphreys and Marcus 2008; Lim et al. 2009). When the relevant atmospheric/geophysical length scales are sufficiently large, both the planar and β-plane approximations break down, and it is necessary to take into account the spherical geometry of the earth/planet. This is discussed in more detail in Newton (2009). The review paper of Aref et al. (2003) highlights the state-of-the-art issues related to equilibrium configurations at the time of publication, before we developed the linear algebra approach for the sphere used in this paper, and in Jamaloodeen and Newton (2006), Newton and Sakajo (2009, 2011). The only paper we know of that investigated relative equilibrium configurations for general (heterogeneous) vortex strengths before that time (aside from the equal and opposite vortex strength configurations produced in vortex street configurations) was that of Lewis and Ratiu (1996). More general vortex distributions on the sphere have also been studied in Crowdy (2004), and also for complex domains on the sphere (Kidambi and Newton 2000; Surana and Crowdy 2008). Stability investigations of configurations on the sphere were initiated by Hally (1980), followed by Borisov and Kilin (2000), Lim et al. (2001), Laurent-Polz (2002), Cabral and Schmidt (1999), Cabral et al. (2003), Boatto and Cabral (2003), and Sakajo (2004).

Our goal in this paper is to combine the linear algebraic techniques initiated in Jamaloodeen and Newton (2006) for the identification of relative equilibria, with nonlinear stability techniques developed by J.E. Marsden and his co-workers over the span of his long and distinguished career.

2 The Icosahedral Configuration as Relative Equilibrium

For definiteness, we focus on the icosahedral configuration shown in Fig. 1, with vortex strengths $\mathbf{\Gamma} = (\Gamma_1, \Gamma_2, \dots, \Gamma_{12}) \in \mathbb{R}^{12}$ placed at the 12 numbered vertices of the icosahedron. Each relative equilibrium configuration of point vortices is a *fixed point* of (1.6). Thus, they are solutions of a system of equations that can be rewritten in the following form:

$$\sum_{k=1, k\neq i, k\neq j}^{N} \frac{\Gamma_k V_{ijk}}{\pi}\left(\frac{1}{l_{jk}^2} - \frac{1}{l_{ik}^2}\right) = 0. \tag{2.1}$$

Since these equations are *linear* in the vortex strength vector, they are best represented as

$$\mathbf{A\Gamma} = 0, \tag{2.2}$$

where $\mathbf{A}$ is an $\frac{N(N-1)}{2} \times N$ matrix with entries $A_{lk} = \frac{V_{ijk}}{\pi}(\frac{1}{l_{jk}^2} - \frac{1}{l_{ik}^2})$, $l = i + j$, $(i, j, k = 1, \dots, N)$ and $\mathbf{\Gamma} = (\Gamma_1, \dots, \Gamma_{12})$, the vector of vortex strengths. From this representation, we immediately see that a given configuration of point vortices on a sphere is a relative equilibrium only if the matrix $\mathbf{A}$ has a nontrivial nullspace.

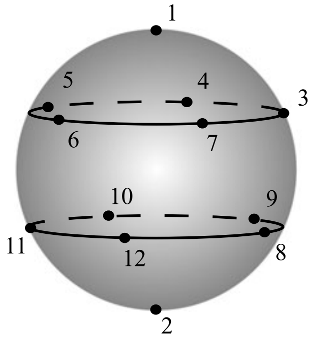

Fig. 1 The numbering convention of the $N = 12$ vertices of the icosahedron at which the point vortices of strength Γ_i $(i = 1, \dots, 12)$ are placed. Vertices 1 and 2 represent the North–South pair, vertices 3–7 represent a Northern latitudinal ring of five evenly spaced vertices, and vertices 8–12 represent a Southern latitudinal ring of five evenly spaced vertices, staggered with respect to the Northern ring. Together, the configuration can be thought of as a special von Kármán vortex street configuration with pole vortices

As was shown in Jamaloodeen and Newton (2006), all the Platonic solids are relative equilibrium configurations for special vortex strength vectors that lie in the appropriate nullspace of the configuration matrix for the given Platonic solid. Thus, if we place vortices at the vertices of an icosahedron, we will get a matrix $\mathbf{A}$ with a nontrivial nullspace. For our purposes in this paper, we choose as the basis set for the nullspace the vectors depicted in Fig. 2. Here, the vector $\mathbf{b}_1 = (1, 1, 1, \dots, 1, 1) \in \mathbb{R}^{12}$ represents the uniform icosahedral configuration, where all point vortex strengths are equal. The other 6 elements $\mathbf{b}_i \in \mathbb{R}^{12}$ $(i = 2, \dots, 7)$ represent equal and opposite strength antipodal vortex pairs placed respectively at vertices 1, 2, vertices 3, 11, vertices 4, 12, vertices 5, 8, vertices 6, 9, and vertices 7, 10.

3 Stability of the Antipodal Basis Elements

The basis vectors $\mathbf{b}_i$ $(2 \le i \le 7)$ represent configurations of vortex pairs located at opposite sides of the sphere (antipodal points) with equal and opposite strengths. The motion of a vortex pair on the sphere is an integrable problem (Newton 2001). To find the solution, consider the equations of motion in vector form:

$$\begin{aligned} \dot{\mathbf{x}}_i &= \frac{\Gamma_j}{2\pi r} \frac{\mathbf{x}_j \times \mathbf{x}_i}{(\mathbf{x}_i - \mathbf{x}_j)^2} = \frac{1}{2\pi r l_{12}^2} (\Gamma_1 \mathbf{x}_1 + \Gamma_2 \mathbf{x}_2) \times \mathbf{x}_i = \frac{1}{2\pi r l_{12}^2} \mathbf{J} \times \mathbf{x}_i, \\ & i = 1, 2,\ j = 1, 2,\ j \neq i, \\ \|x_i\|^2 &= r^2, \quad i = 1, 2. \end{aligned} \tag{3.1}$$

From (1.6) we have

$$\frac{\mathrm{d} l_{12}^2}{\mathrm{d}t} = 0.$$

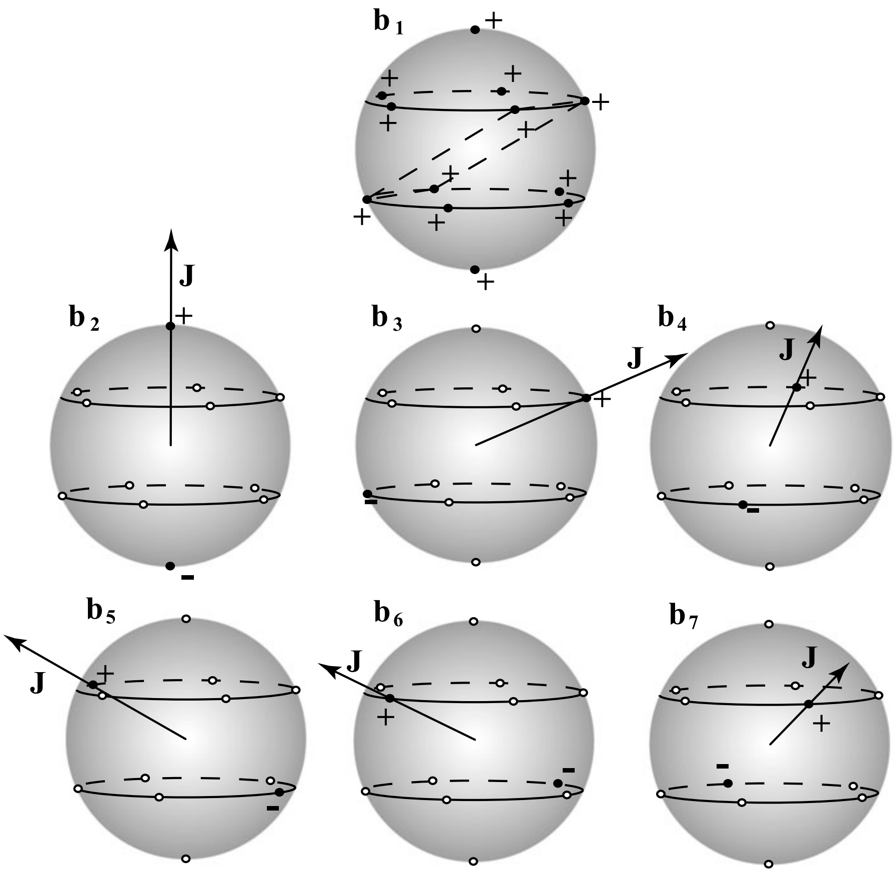

Fig. 2 Nullspace basis set of the configuration matrix for the icosahedron. $\mathbf{b}_1$ represents the uniform icosahedron, while $\mathbf{b}_2$–$\mathbf{b}_7$ represent antipodal equal and opposite strength pairs

Thus $l_{12}^2 = \text{const.}$ and (3.1) describe rotations of $\mathbf{x}_i$, $i = 1, 2$ around the constant vector $\frac{1}{2\pi r l_{12}^2}\mathbf{J}$. From this, we have the theorem:

Theorem 3.1 *The antipodal vortex pair configuration* ($\mathbf{x}_1 = -\mathbf{x}_2$, $\Gamma_1 = -\Gamma_2$) *is a stable equilibrium configuration.*

Proof By adding small perturbations $\delta\mathbf{x}_1$ and $\delta\mathbf{x}_2$ to the given configuration (see Fig. 3 for details), we get a configuration that will rotate around fixed vector $\tilde{\mathbf{J}} = \Gamma_1(\mathbf{x}_1 + \delta\mathbf{x}_1) + \Gamma_2(\mathbf{x}_2 + \delta\mathbf{x}_2)$ and thus will stay within a spherical cap centered at $\mathbf{x}_1, \mathbf{x}_2$ with angular radius α equal to

$$\alpha = \cos^{-1}\left(\frac{\tilde{\mathbf{J}} \cdot \mathbf{J}}{\|\tilde{\mathbf{J}}\| \|\mathbf{J}\|}\right) + \max\left\{\cos^{-1}\left(\frac{\tilde{\mathbf{J}} \cdot (\mathbf{x}_i + \delta\mathbf{x}_i)}{\|\tilde{\mathbf{J}}\| \|\mathbf{x}_i + \delta\mathbf{x}_i\|}\right) \middle| i = 1, 2\right\}.$$

Notice that for any two perturbations $\delta\mathbf{x}_1, \delta\mathbf{x}_2$, from a spherical cap with radius α, vectors $\tilde{\mathbf{J}}, \mathbf{J}$ will stay inside one cap with radius α. Thus, for any $\varepsilon > 0$, there exists

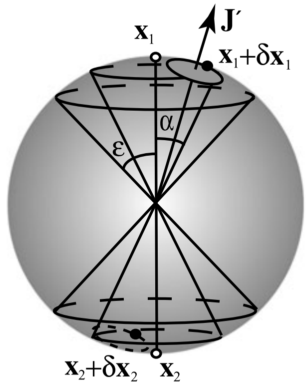

Fig. 3 Antipodal vortex pair $(\mathbf{x}_1, \mathbf{x}_2)$ under perturbation $(\mathbf{x}_1 + \delta\mathbf{x}_1, \mathbf{x}_2 + \delta\mathbf{x}_2)$. The perturbed pair will oscillate around $\mathbf{J}'$, making the antipodal pair nonlinearly stable

$\alpha = \varepsilon/3 > 0$, such that for any perturbations $\delta\mathbf{x}_1, \delta\mathbf{x}_2$ from spherical caps centered at $\mathbf{x}_1, \mathbf{x}_2$ with angular radius α, the perturbed system will stay within spherical caps centered at $\mathbf{x}_1, \mathbf{x}_2$ with radius ε. □

4 Stability Regions for the General Icosahedron

The classical definition of stability is due to Routh and is described in detail in Marsden and Ratiu (1999). A relative equilibrium is stable if it is *Lyapunov stable* on a reduced space in which the relative equilibrium is a fixed point. The energy-momentum method is designed to prove stability of relative equilibria on the unreduced space (see Simo et al. 1991). According to the method, in order to conclude stability, one has to consider a subspace P_1 of a tangent space to the level set of the momentum map at the equilibrium, where the neutrally stable directions have been eliminated. In the context of point vortex dynamics, a relative equilibrium is stable in the Routh sense if the *energy-momentum functional* (relative Hamiltonian in terms of Kurakin 2004)

$$\begin{aligned} H_{\mu_e}(z, \xi) &= H(z) - \big(\mathbf{J}(z) - \mu_e\big) \cdot \omega, \\ \mu_e &= \mathbf{J}(z_e), \end{aligned} \tag{4.1}$$

attains its strict minimum (or maximum) on the space P_1. According to Patrick's theorem (see Patrick 1992), if the second variation of the energy-momentum functional is positive (or negative) definite, and the action of the isotropy subgroup is proper, and the Lie algebra admits an inner product invariant under the adjoint action of the isotropy subgroup, then the relative equilibrium is stable modulo the isotropy subgroup. Note that in our case the isotropy subgroup is a compact group SO(3); thus all of the assumptions of Patrick's theorem are automatically satisfied.

If $\mathbf{J}$ is aligned with the z-axis, the energy-momentum functional in the mixed chart introduced in the previous sections can be written as

$$H_{\mu_e} = H_m - \omega\left(\sum_{i=1}^{N} \Gamma_i z_i - \Gamma_s\sqrt{r^2 - x_{1,s}^2 - y_{1,s}^2} + \Gamma_n\sqrt{r^2 - x_{1,n}^2 - y_{1,n}^2}\right). \tag{4.2}$$

Notice that, by plugging in H_{μ_e} in Hamilton's equations instead of H, we will get the equations of motion in a coordinate system which rotates about axis z with angular velocity ω. In this coordinate system, the relative equilibrium becomes a stationary equilibrium.

To get an instability result, we use the Lyapunov instability criterion. According to this criterion, the system is *nonlinearly unstable* if it is *linearly unstable*. For this, consider the general Hamiltonian system in canonical variables

$$\dot{p} = \frac{\partial H}{\partial q},$$
$$\dot{q} = -\frac{\partial H}{\partial p}.$$

Its linearization about an equilibrium (p_e, q_e) can be written as

$$\dot{\delta p} = \left.\frac{\partial^2 H}{\partial q \partial p}\right|_{(p_e,q_e)} \delta p + \left.\frac{\partial^2 H}{\partial q^2}\right|_{(p_e,q_e)} \delta q,$$
$$\dot{\delta q} = -\left.\frac{\partial^2 H}{\partial p^2}\right|_{(p_e,q_e)} \delta p - \left.\frac{\partial^2 H}{\partial p \partial q}\right|_{(p_e,q_e)} \delta q,$$

where $p = p_e + \delta p, q = q_e + \delta q$. The previous equations can be rewritten in the following matrix form:

$$\frac{\mathrm{d}}{\mathrm{d}t}\begin{pmatrix} \delta p \\ \delta q \end{pmatrix} = \begin{pmatrix} \mathbf{0} & \mathbf{I} \\ -\mathbf{I} & \mathbf{0} \end{pmatrix} \begin{pmatrix} \frac{\partial^2 H}{\partial p^2} & \frac{\partial^2 H}{\partial p \partial q} \\ \frac{\partial^2 H}{\partial q \partial p} & \frac{\partial^2 H}{\partial q^2} \end{pmatrix} \begin{pmatrix} \delta p \\ \delta q \end{pmatrix} = \boldsymbol{\Omega} D^2 H \begin{pmatrix} \delta p \\ \delta q \end{pmatrix}. \tag{4.3}$$

To conclude *instability*, we have to show that $\boldsymbol{\Omega} D^2 H_{\mu_e}$ has eigenvalues with positive real parts.

To simplify the computations (i.e., reduce the parameter space) and to visualize the regions of stability, we study the stability of the superposition of the three key configurations shown in Fig. 4, namely the (i) uniform icosahedron, (ii) the von Kármán street configuration, and (iii) the North–South vortex pair. Since the configurations are axisymmetric, we use cylindrical coordinates aligned with vector $\mathbf{J}$. If we choose our coordinates of the vertices of the icosahedron in the form

$$\begin{aligned} &\mathbf{x}_1 = (0, 0, 1), \qquad \mathbf{x}_2 = (0, 0, -1), \\ &\mathbf{x}_{i+3} = \left(\frac{2}{\sqrt{5}} \cos \frac{2\pi i}{5}, \frac{2}{\sqrt{5}} \sin \frac{2\pi}{5}, \frac{1}{\sqrt{5}}\right), \quad i = 0, \dots, 4, \\ &\mathbf{x}_{i+8} = \left(\frac{2}{\sqrt{5}} \cos \frac{\pi + 2\pi i}{5}, \frac{2}{\sqrt{5}} \sin \frac{\pi + 2\pi}{5}, -\frac{1}{\sqrt{5}}\right), \quad i = 0, \dots, 4, \end{aligned} \tag{4.4}$$

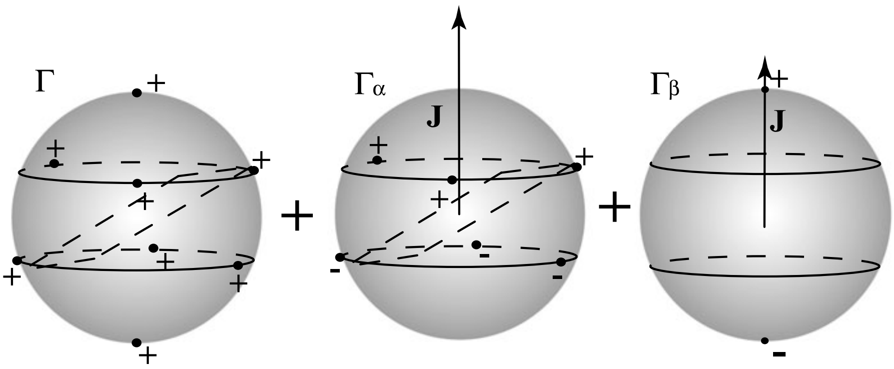

Fig. 4 Creation of the general icosahedron via superposition using the three parameters: $(\Gamma, \Gamma_\alpha, \Gamma_\beta)$. (i) $(1,0,0)$ the uniform icosahedron; (ii) $(0,1,0)$ a von Kármán vortex street; (iii) $(0,0,1)$ a North–South polar pair. Stability is analyzed as a function of these three parameters

and then use a symmetry induced basis[1] for the space P_1 (see Serre 1977), we get the following matrix of second variation:

$$D^2 H_{\mu_e}|_{P_1} = \begin{pmatrix} -8(\Gamma^2-\Gamma_\alpha^2) & 0 & 0 & 0 \\ 0 & -\frac{25}{2}(\Gamma^2-\Gamma_\alpha^2)(10\Gamma^2-\Gamma_\alpha(4\Gamma_\alpha+\sqrt{5}\Gamma_\beta)) & 0 & 0 \\ 0 & 0 & \mathbf{C} & 0 \\ 0 & 0 & 0 & \mathbf{D} \end{pmatrix}, \tag{4.5}$$

where $\mathbf{C}$ is an 8×8 matrix and $\mathbf{D}$ is a 10×10 matrix whose entries can be found in the Appendix.

Since matrix $D^2 H_{\mu_e}|_{P_1}$ has to be definite, using the Sylvester criterion (Meyer 2000) we get

$$\begin{aligned}
&\big(10\Gamma^2-\Gamma_\alpha(4\Gamma_\alpha+\sqrt{5}\Gamma_\beta)\big) > 0,\\
&-8\big(\Gamma^2-\Gamma_\alpha^2\big)\mathbf{C}_{1,1} > 0,\\
&-8\big(\Gamma^2-\Gamma_\alpha^2\big)\mathbf{D}_{1,1} > 0,\\
&\mathbf{C}_{1,1}\mathbf{C}_{2i-1,2i-1} > 0,\\
&\mathbf{C}_{2i,2i} > 0, \quad i=1,\dots,4,\\
&\mathbf{D}_{1,1}\mathbf{D}_{2i-1,2i-1} > 0,\\
&\mathbf{D}_{2i,2i} > 0, \quad i=1,\dots,5,
\end{aligned}$$

where $\mathbf{C}_{i,i}$ is the ith principal minor of $\mathbf{C}$. Visualizations of these conditions are given in the plots shown in Figs. 5 and 6.

[1] A symmetry induced basis is a basis of the invariant subspaces of the dihedral group D_5 (symmetry group of regular 5-gon). As such, it is the biggest symmetry subgroup of the configuration under investigation; i.e., the configuration will not change if we do cyclic rotations by an angle $\frac{2\pi}{5}$ about the z-axis or flip about any plane which goes through the z-axis and any vertex.

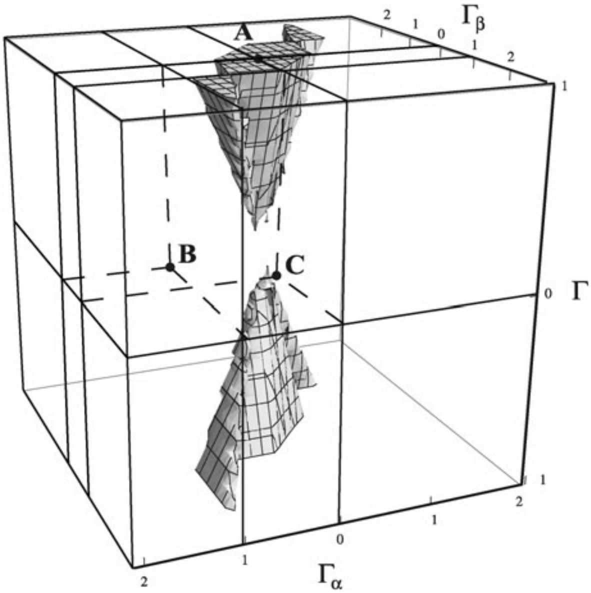

Fig. 5 Regions of stability for icosahedral configurations. Individual grouped component points are marked as $A : (\Gamma, \Gamma_\alpha, \Gamma_\beta) = (1, 0, 0)$, $B : (\Gamma, \Gamma_\alpha, \Gamma_\beta) = (0, 1, 0)$, $C : (\Gamma, \Gamma_\alpha, \Gamma_\beta) = (0, 0, 1)$

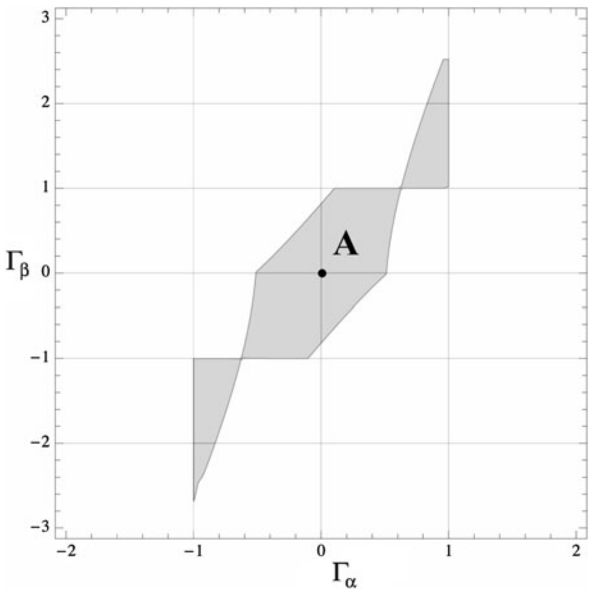

Fig. 6 Plane $\Gamma = 1$. *Shaded region* is the stable region. *Point A* corresponds to the uniform icosahedron

Notice that the uniform icosahedral configuration (point A) $(\Gamma, \Gamma_\alpha, \Gamma_\beta) = (1, 0, 0)$ is a stable relative equilibrium configuration, as first derived in Kurakin (2004). Also note that because of (2.2), we can scale all the vortex strengths equally, and we retain the equilibrium. This implies that the shaded stable regions for each slice of Γ (shown in Fig. 6 for $\Gamma = 1$), all have the same shape, modulo rescaling. So, as Γ increases, the region of stability opens up, which indicates that the stability of the uniform icosahedron can be used to *stabilize* the relative equilibrium, if we choose Γ sufficiently large.

The configuration $(\Gamma, \Gamma_\alpha, \Gamma_\beta) = (0, 0, 1)$ (point C) is a polar vortex pair and, as we have proven above, it is a stable configuration. Notice that we proved this by direct methods. The energy-momentum method used for this configuration gives no conclusive information on stability, as the second variation on the space P_1 has zero eigenvalues (i.e., the configuration is degenerate). That is why point C does not lie in a shaded region of the figure, despite the fact that it is stable. The von Kármán configuration $(\Gamma, \Gamma_\alpha, \Gamma_\beta) = (0, 1, 0)$ (point B), as shown below, is unstable.

Theorem 4.1 *The von Kármán relative equilibrium configuration* $(\Gamma, \Gamma_\alpha, \Gamma_\beta) = (0, 1, 0)$ *is linearly unstable.*

Proof If we multiply the matrix of second variation of the Hamiltonian by the inverse of the symplectic form, then we can find the eigenvalues of linearized system,

$$-1.98083, 1.98083, 1.98083, -1.98083, 1.86933i, -1.86933i, 1.86933i,$$

$$-1.86933i, 1.43418, -1.43418, -1.43418, 1.43418, 1.32288i, -1.32288i,$$

$$-0.513637, 0.513637, 0.513637, -0.513637, 0, 0.$$

As we can see, there are six of them with positive real part. Thus, the configuration is linearly unstable. □

5 Discussion

The results in this paper describe the stability and instability of the icosahedral point vortex relative equilibrium configuration for general vortex strengths when the strengths are grouped according to the groupings shown in Fig. 4, namely the uniform icosahedron, a special von Kármán vortex street, and the North–South antipodal pairing of equal and opposite vortices. These groupings are chosen because of their physical relevance, but the fact that, when linearly combined, they remain in relative equilibrium follows from the nullspace structure of the configuration matrix **A**. The stability of each of these configurations can be treated separately using the augmented Hamiltonian, as described in the text, but this does not provide any insight into their stability when they are linearly combined.

Some key points are worth emphasizing. The regions of stability are shown in Fig. 5 for the three parameters $(\Gamma, \Gamma_\alpha, \Gamma_\beta)$, and a special slice of this space $(\Gamma = 1)$ is shown in Fig. 6. One can see that, because the region of stability opens up for increasing Γ (Fig. 5), in some sense, the uniform icosahedron acts as a stabilizing influence on the system. For any given values of $(\Gamma_\alpha, \Gamma_\beta)$, for large enough Γ, the point $(\Gamma, \Gamma_\alpha, \Gamma_\beta)$ will lie in the stable region. Whether or not the special equal strength choice stabilizes the other Platonic solid relative equilibria is not known at this point (see Jamaloodeen and Newton 2006).

We finish by mentioning that icosahedral configurations of interacting "particle" systems, and more complex configurations that possess icosahedral symmetry, have been investigated extensively in the literature associated with the structure of virus molecules (a relatively recent contribution is that of Zandi et al. 2004). We believe the general nullspace decomposition and stability approach described in this paper could be applied in that context as well.

Acknowledgements We dedicate this paper to the memory of Jerry Marsden, whose work in Hamiltonian mechanics and stability theory laid the groundwork for much that is described in this paper. Support from the National Science Foundation, grant NSF-DMS-0804629, is greatly appreciated.

Appendix

Matrix **C** can be written as

$$\mathbf{C} = \begin{pmatrix} C_1 & C_2 & C_3 & C_4 \\ C_2 & C_5 & C_6 & C_7 \\ C_3 & C_6 & C_8 & C_9 \\ C_4 & C_8 & C_9 & C_{10} \end{pmatrix},$$

where $C_i, i = 1, \dots, 10$ are 2×2 matrices:

$$C_1 = \begin{pmatrix} -\frac{1}{8}(\Gamma + \Gamma_\alpha)(203\Gamma + 37\Gamma_\alpha + 25\sqrt{5}\Gamma_\beta) & 0 \\ 0 & -\frac{1}{8}(\Gamma + \Gamma_\alpha)(203\Gamma + 37\Gamma_\alpha + 25\sqrt{5}\Gamma_\beta) \end{pmatrix},$$

$$C_2 = \begin{pmatrix} \frac{27}{128}(-1+\sqrt{5})(\Gamma^2 - \Gamma_\alpha^2) & \frac{1}{128}\sqrt{2643290 + 922258\sqrt{5}}(\Gamma_\alpha^2 - \Gamma^2) \\ \frac{1}{128}\sqrt{1659290 - 61742\sqrt{5}}(\Gamma_\alpha^2 - \Gamma^2) & \frac{27}{128}(-1+\sqrt{5})(\Gamma^2 - \Gamma_\alpha^2) \end{pmatrix},$$

$$C_3 = \begin{pmatrix} \frac{1}{8}(\Gamma + \Gamma_\alpha)(53\Gamma + 187\Gamma_\alpha - 25\sqrt{5}\Gamma_\beta) & 0 \\ 0 & -\frac{1}{8}(\Gamma + \Gamma_\alpha)(53\Gamma + 187\Gamma_\alpha - 25\sqrt{5}\Gamma_\beta) \end{pmatrix},$$

$$C_4 = \begin{pmatrix} \frac{1}{128}(877 - 77\sqrt{5})(\Gamma^2 - \Gamma_\alpha^2) & \frac{27}{64}\sqrt{\frac{1}{2}(5+\sqrt{5})}(\Gamma^2 - \Gamma_\alpha^2) \\ \frac{27}{64}\sqrt{\frac{1}{2}(5+\sqrt{5})}(\Gamma^2 - \Gamma_\alpha^2) & \frac{1}{128}(1123 - 323\sqrt{5})(\Gamma^2 - \Gamma_\alpha^2) \end{pmatrix},$$

$$C_5 = \begin{pmatrix} -\frac{1}{8}(\Gamma - \Gamma_\alpha)(203\Gamma - 37\Gamma_\alpha - 25\sqrt{5}\Gamma_\beta) & 0 \\ 0 & -\frac{1}{8}(\Gamma - \Gamma_\alpha)(203\Gamma - 37\Gamma_\alpha - 25\sqrt{5}\Gamma_\beta) \end{pmatrix},$$

$$C_6 = \begin{pmatrix} \frac{1}{128}(-1123 + 323\sqrt{5})(\Gamma^2 - \Gamma_\alpha^2) & -\frac{27}{64}\sqrt{\frac{1}{2}(5+\sqrt{5})}(\Gamma^2 - \Gamma_\alpha^2) \\ -\frac{27}{64}\sqrt{\frac{1}{2}(5+\sqrt{5})}(\Gamma^2 - \Gamma_\alpha^2) & \frac{1}{128}(-877 + 77\sqrt{5})(\Gamma^2 - \Gamma_\alpha^2) \end{pmatrix},$$

$$C_7 = \begin{pmatrix} \frac{1}{8}(\Gamma - \Gamma_\alpha)(53\Gamma - 187\Gamma_\alpha + 25\sqrt{5}\Gamma_\beta) & 0 \\ 0 & -\frac{1}{8}(\Gamma - \Gamma_\alpha)(53\Gamma - 187\Gamma_\alpha + 25\sqrt{5}\Gamma_\beta) \end{pmatrix},$$

$$C_8 = \begin{pmatrix} -\frac{1}{8}(\Gamma + \Gamma_\alpha)(203\Gamma + 37\Gamma_\alpha + 25\sqrt{5}\Gamma_\beta) & 0 \\ 0 & -\frac{1}{8}(\Gamma + \Gamma_\alpha)(203\Gamma + 37\Gamma_\alpha + 25\sqrt{5}\Gamma_\beta) \end{pmatrix},$$

$$C_9 = \begin{pmatrix} \frac{27}{128}(-1+\sqrt{5})(\Gamma^2 - \Gamma_\alpha^2) & \frac{1}{128}\sqrt{1659290 - 61742\sqrt{5}}(\Gamma_\alpha^2 - \Gamma^2) \\ \frac{1}{128}\sqrt{2643290 + 922258\sqrt{5}}(\Gamma_\alpha^2 - \Gamma^2) & \frac{27}{128}(-1+\sqrt{5})(\Gamma^2 - \Gamma_\alpha^2) \end{pmatrix},$$

$$C_{10} = \begin{pmatrix} -\frac{1}{8}(\Gamma - \Gamma_\alpha)(203\Gamma - 37\Gamma_\alpha - 25\sqrt{5}\Gamma_\beta) & 0 \\ 0 & -\frac{1}{8}(\Gamma - \Gamma_\alpha)(203\Gamma - 37\Gamma_\alpha - 25\sqrt{5}\Gamma_\beta) \end{pmatrix}.$$

Matrix **D** can be written as

$$\mathbf{D} = \begin{pmatrix} D_1 & D_2 & D_3 & D_4 & D_5 \\ D_2 & D_6 & D_7 & D_8 & D_9 \\ D_3 & D_7 & D_{10} & D_{11} & D_{12} \\ D_4 & D_8 & D_{11} & D_{13} & D_{14} \\ D_5 & D_9 & D_{12} & D_{14} & D_{15} \end{pmatrix},$$

where $D_i, i = 1, \dots, 15$ are 2×2 matrices:

$$D_1 = \begin{pmatrix} -\frac{5}{8}(\Gamma + \Gamma_\alpha)(33\Gamma + 2\Gamma_\alpha + 5\sqrt{5}\Gamma_\beta) & 0 \\ 0 & -\frac{5}{8}(\Gamma + \Gamma_\alpha)(33\Gamma + 2\Gamma_\alpha + 5\sqrt{5}\Gamma_\beta) \end{pmatrix},$$

$$D_2 = \begin{pmatrix} -\frac{5}{16}(1 + \sqrt{5})(\Gamma^2 - \Gamma_\alpha^2) & \frac{5(\Gamma^2 - \Gamma_\alpha^2)}{4\sqrt{2 + \frac{2}{\sqrt{5}}}} \\ \frac{5(\Gamma_\alpha^2 - \Gamma^2)}{4\sqrt{2 + \frac{2}{\sqrt{5}}}} & -\frac{5}{16}(1 + \sqrt{5})(\Gamma^2 - \Gamma_\alpha^2) \end{pmatrix},$$

$$D_3 = \begin{pmatrix} 0 & -\frac{25(\Gamma^2 - \Gamma_\alpha^2)(5((5+\sqrt{5})\Gamma + (1+\sqrt{5})\Gamma_\beta) - (5+\sqrt{5})\Gamma_\alpha)}{2(5+\sqrt{5})} \\ -\frac{25(\Gamma^2 - \Gamma_\alpha^2)(5((5+\sqrt{5})\Gamma + (1+\sqrt{5})\Gamma_\beta) - (5+\sqrt{5})\Gamma_\alpha)}{2(5+\sqrt{5})} & 0 \end{pmatrix},$$

$$D_4 = \begin{pmatrix} c & 0 \\ 0 & d \end{pmatrix},$$

$$c = -\frac{5}{8}(\Gamma + \Gamma_\alpha)(\Gamma + \Gamma_\beta)\big(3(9 + \sqrt{5})\Gamma + 3(1 + \sqrt{5})\Gamma_\alpha + 4\sqrt{5}\Gamma_\beta\big),$$

$$d = \frac{5(\Gamma + \Gamma_\alpha)(\Gamma - \Gamma_\beta)((33 + 9\sqrt{5})\Gamma - 3(1 + \sqrt{5})\Gamma_\alpha + 2(5 + 3\sqrt{5})\Gamma_\beta)}{4(3 + \sqrt{5})},$$

$$D_5 = \begin{pmatrix} \frac{15}{4}\sqrt{5}(\Gamma + \Gamma_\alpha)(\Gamma^2 - \Gamma_\beta^2) & 0 \\ 0 & \frac{15}{4}\sqrt{5}(\Gamma + \Gamma_\alpha)(\Gamma^2 - \Gamma_\beta^2) \end{pmatrix},$$

$$D_6 = \begin{pmatrix} -\frac{5}{8}(\Gamma - \Gamma_\alpha)(33\Gamma - 2\Gamma_\alpha - 5\sqrt{5}\Gamma_\beta) & 0 \\ 0 & -\frac{5}{8}(\Gamma - \Gamma_\alpha)(33\Gamma - 2\Gamma_\alpha - 5\sqrt{5}\Gamma_\beta) \end{pmatrix},$$

$$D_7 = \begin{pmatrix} e & f \\ f & e \end{pmatrix},$$

$$e = -\frac{25}{8}\sqrt{10 - 2\sqrt{5}}\big(\Gamma^2 - \Gamma_\alpha^2\big)(5\Gamma + \Gamma_\alpha - \sqrt{5}\Gamma_\beta),$$

$$f = -\frac{25(\Gamma^2 - \Gamma_\alpha^2)(5(5 + 3\sqrt{5})\Gamma + (5 + 3\sqrt{5})\Gamma_\alpha - 5(3 + \sqrt{5})\Gamma_\beta)}{4(5 + \sqrt{5})},$$

$$D_8 = \begin{pmatrix} \frac{5}{8}(-2+\sqrt{5})(\Gamma^2-\Gamma_\alpha^2)(\Gamma+\Gamma_\beta) & -\frac{5}{16}\sqrt{130+58\sqrt{5}}(\Gamma^2-\Gamma_\alpha^2)(\Gamma-\Gamma_\beta) \\ -\frac{5}{8}\sqrt{85-38\sqrt{5}}(\Gamma^2-\Gamma_\alpha^2)(\Gamma+\Gamma_\beta) & -\frac{5}{16}(11+5\sqrt{5})(\Gamma^2-\Gamma_\alpha^2)(\Gamma-\Gamma_\beta) \end{pmatrix},$$

$$D_9 = \begin{pmatrix} \frac{15}{16}(5+\sqrt{5})(\Gamma-\Gamma_\alpha)(\Gamma^2-\Gamma_\beta^2) & \frac{15}{16}\sqrt{50-10\sqrt{5}}(\Gamma-\Gamma_\alpha)(\Gamma^2-\Gamma_\beta^2) \\ -\frac{75(\Gamma-\Gamma_\alpha)(\Gamma^2-\Gamma_\beta^2)}{4\sqrt{2(5+\sqrt{5})}} & \frac{15}{16}(5+\sqrt{5})(\Gamma-\Gamma_\alpha)(\Gamma^2-\Gamma_\beta^2) \end{pmatrix},$$

$$D_{10} = \begin{pmatrix} -25(\Gamma^2-\Gamma_\alpha^2)(15\Gamma^2+9\Gamma_\alpha^2-4\sqrt{5}\Gamma_\alpha\Gamma_\beta) & 0 \\ 0 & -25(\Gamma^2-\Gamma_\alpha^2)(15\Gamma^2+9\Gamma_\alpha^2-4\sqrt{5}\Gamma_\alpha\Gamma_\beta) \end{pmatrix},$$

$$D_{11} = \begin{pmatrix} 0 & g \\ h & 0 \end{pmatrix},$$

$$g = \frac{10(\Gamma^2-\Gamma_\alpha^2)(\Gamma-\Gamma_\beta)(5(-5+2\sqrt{5})\Gamma+(5+4\sqrt{5})\Gamma_\alpha-5(-1+\sqrt{5})\Gamma_\beta)}{-5+\sqrt{5}},$$

$$h = \frac{5(\Gamma^2-\Gamma_\alpha^2)(\Gamma+\Gamma_\beta)((-35+17\sqrt{5})\Gamma_\alpha+5((5+\sqrt{5})\Gamma+2(-1+\sqrt{5})\Gamma_\beta))}{-5+\sqrt{5}},$$

$$D_{12} = \begin{pmatrix} 0 & 25\sqrt{5}(\Gamma^2-\Gamma_\alpha^2)(\Gamma^2-\Gamma_\beta^2) \\ 25\sqrt{5}(\Gamma^2-\Gamma_\alpha^2)(\Gamma^2-\Gamma_\beta^2) & 0 \end{pmatrix},$$

$$D_{13} = \begin{pmatrix} k & 0 \\ 0 & l \end{pmatrix},$$

$$k = -\frac{1}{2}(\Gamma+\Gamma_\alpha)(\Gamma+\Gamma_\beta)\big((38+5\sqrt{5})\Gamma^2 + (31+9\sqrt{5})\Gamma_\beta\Gamma+5\sqrt{5}\Gamma_\alpha^2+4\sqrt{5}\Gamma_\beta^2+(7+5\sqrt{5})\Gamma_\alpha(2\Gamma+\Gamma_\beta)\big),$$

$$l = \frac{1}{4(3+\sqrt{5})}(\Gamma+\Gamma_\alpha)(\Gamma-\Gamma_\beta)\big(-2(89+23\sqrt{5})\Gamma^2+10(5+3\sqrt{5})\Gamma_\alpha^2 + 8(1+2\sqrt{5})\Gamma_\alpha(2\Gamma-\Gamma_\beta)+8\Gamma_\beta\big((12+\sqrt{5})\Gamma+(5+3\sqrt{5})\Gamma_\beta\big)\big),$$

$$D_{14} = \begin{pmatrix} m & 0 \\ 0 & n \end{pmatrix},$$

$$m = -\frac{(\Gamma+\Gamma_\alpha)(5(1+\sqrt{5})\Gamma+5(-5+3\sqrt{5})\Gamma_\alpha+4(-4+3\sqrt{5})\Gamma_\beta)(\Gamma^2-\Gamma_\beta^2)}{2(-3+\sqrt{5})},$$

$$n = \frac{(\Gamma+\Gamma_\alpha)(5(-11+5\sqrt{5})\Gamma+5(-5+3\sqrt{5})\Gamma_\alpha+2(17-9\sqrt{5})\Gamma_\beta)(\Gamma^2-\Gamma_\beta^2)}{2(-3+\sqrt{5})},$$

$$D_{15} = \begin{pmatrix} -(10\Gamma^2-3\Gamma_\beta^2-5\sqrt{5}\Gamma_\alpha\Gamma_\beta)(\Gamma^2-\Gamma_\beta^2) & 0 \\ 0 & -(10\Gamma^2-3\Gamma_\beta^2-5\sqrt{5}\Gamma_\alpha\Gamma_\beta)(\Gamma^2-\Gamma_\beta^2) \end{pmatrix}.$$

References

Aref, H., Newton, P.K., Stremler, M.A., Tokieda, T., Vainchtein, D.L.: Vortex crystals. Adv. Appl. Mech. **39**, 1–79 (2003)

Boatto, S., Cabral, H.E.: Non-linear stability of a latitudinal ring of point vortices on a non-rotating sphere. SIAM J. Appl. Math. **64**(1), 216–230 (2003)

Bogomolov, V.A.: Dynamics of the vorticity on a sphere. Izv. Akad. Nauk SSSR Mekh. Zhidk. Gaza, pp. 57–65 (1977)

Borisov, A.V., Kilin, A.A.: Stability of Thomson's configurations of vortices on a sphere. Regul. Chaotic Dyn. **5**, 189–200 (2000)

Cabral, H.E., Schmidt, D.S.: Stability of relative equilibria in the problem of $N+1$ vortices. SIAM J. Math. Anal. **31**(2), 231–250 (1999)

Cabral, H.E., Meyer, K.R., Schmidt, D.S.: Stability and bifurcations for the $N+1$ vortex problem on the sphere. Regul. Chaotic Dyn. **8**(3), 259–282 (2003)

Chamoun, G., Kanso, E., Newton, P.K.: Von Kármán vortex streets on a sphere. Phys. Fluids **21**, 116603 (2009)

Crowdy, D.G.: Stuart vortices on a sphere. J. Fluid Mech. **498**, 381–402 (2004)

Hally, D.: Stability of streets of vortices on surfaces of revolution with a reflection symmetry. J. Math. Phys. **21**, 211 (1980)

Humphreys, T., Marcus, P.S.: Vortex street dynamics: the selection mechanism for the areas and locations of Jupiter's vortices. J. Atmos. Sci. **64**, 1318–1333 (2008)

Jamaloodeen, M.I., Newton, P.K.: The N-vortex problem on a rotating sphere. II. Heterogeneous Platonic solid equilibria. Proc. R. Soc. A, Math. Phys. Eng. Sci. **462**(2075), 3277 (2006)

Kidambi, R., Newton, P.K.: Motion of three point vortices on a sphere. Physica D **116**, 143–175 (1998)

Kidambi, R., Newton, P.K.: Point vortex motion on a sphere with solid boundaries. Phys. Fluids **12**(3), 581–588 (2000)

Kimura, Y., Okamoto, H.: Vortex motion on a sphere. J. Phys. Soc. Jpn. **56**, 4203–4206 (1987)

Kurakin, L.G.: On nonlinear stability of the regular vortex systems on a sphere. Chaos **14**(3), 592–602 (2004)

Laurent-Polz, F.: Point vortices on the sphere: a case with opposite vortices. Nonlinearity **15**, 143–171 (2002)

Lewis, D., Ratiu, T.: Rotating n-gon/kn-gon vortex configurations. J. Nonlinear Sci. **6**, 385–414 (1996)

Lim, C.C., Montaldi, J., Roberts, M.R.: Relative equilibria of point vortices on a sphere. Physica D **148**, 97–135 (2001)

Lim, C.C., Ding, X., Nebus, J.: Vorticity Dynamics, Statistical Mechanics, and Planetary Atmospheres. World Scientific, Singapore (2009)

Marsden, J.E., Ratiu, T.S.: Introduction to Mechanics and Symmetry, 2nd edn. Texts in Applied Mathematics, vol. 17. Springer, New York (1999)

Meyer, C.D.: Matrix Analysis and Applied Linear Algebra. Society for Industrial Mathematics, Philadelphia (2000)

Newton, P.K.: The N-Vortex Problem. Analytical Techniques. Applied Mathematical Sciences, vol. 145. Springer, New York (2001)

Newton, P.K.: The N-vortex problem on a sphere: geophysical mechanisms that break integrability. Theor. Comput. Fluid Dyn. (2009). doi:10.1007/s00162-009-0109-6

Newton, P.K., Sakajo, T.: Point vortex equilibria on the sphere via Brownian ratchets. Proc. R. Soc. A **465**(2102), 437 (2009)

Newton, P.K., Sakajo, T.: Point vortex equilibria and optimal packings of circles on a sphere. Proc. R. Soc. A **467**(2102), 1468–1490 (2011)

Patrick, G.: Relative equilibria in Hamiltonian systems: the dynamic interpretation of nonlinear stability on a reduced phase space. J. Geom. Phys. **9**, 111–119 (1992)

Pekarsky, S., Marsden, J.E.: Point vortices on a sphere: stability of relative equilibria. J. Math. Phys. **39**(11), 5894–5907 (1998)

Polvani, L.M., Dritschel, D.G.: Wave and vortex dynamics on the surface of a sphere. J. Fluid Mech. **255**, 35–64 (1993)

Sakajo, T.: Transition of global dynamics of a polygonal vortex ring on a sphere with pole vortices. Physica D **196**, 243–264 (2004)

Serre, J.P.: Linear Representations of Finite Groups. Springer, New York (1977)

Simo, J.C., Lewis, D., Marsden, J.E.: Stability of relative equilibria. Part I: the reduced energy-momentum method. Arch. Ration. Mech. Anal. **115**(1), 15–59 (1991)

Surana, A., Crowdy, D.G.: Vortex dynamics in a complex domain on a spherical surface. J. Comput. Phys. **227**, 6058–6070 (2008)

Zandi, R., Reguera, D., Bruinsma, R.F., Gelbart, W.M., Rudnick, J.: Origin of icosahedral symmetry in viruses. Proc. Natl. Acad. Sci. USA **101**, 15556–15560 (2004)